

Exploring the Potential of Short-Baseline Physics at Fermilab

O. G. Miranda ^{1,*}, Pedro Pasquini ^{2,†}, M. Tórtola ^{3,‡} and J. W. F. Valle ^{3§}

¹ *Departamento de Física, Centro de Investigación y de Estudios Avanzados del IPN
Apdo. Postal 14-740 07000 Mexico, DF, Mexico*

² *Instituto de Física Gleb Wataghin - UNICAMP, 13083-859, Campinas SP, Brazil and*

³ *AHEP Group, Institut de Física Corpuscular –
C.S.I.C./Universitat de València, Parc Científic de Paterna.
C/Catedrático José Beltrán, 2 E-46980 Paterna (València) - SPAIN*

Abstract

We study the capabilities of the short baseline neutrino program at Fermilab to probe the unitarity of the lepton mixing matrix. We find the sensitivity to be slightly better than the current one. Motivated by the future DUNE experiment, we have also analyzed the potential of an extra liquid Argon near detector in the LBNF beamline. Adding such a near detector to the DUNE setup will substantially improve the current sensitivity on non-unitarity. This would help to remove CP degeneracies due to the new complex phase present in the neutrino mixing matrix. We also study the sensitivity of our proposed setup to light sterile neutrinos for various configurations.

PACS numbers: 13.15.+g, 14.60.Pq, 14.60.St, 23.40.Bw

*Electronic address: omr@fis.cinvestav.mx

†Electronic address: pasquini@ifi.unicamp.br

‡Electronic address: mariam@ific.uv.es

§Electronic address: valle@ific.uv.es, URL: <http://astroparticles.es/>

I. INTRODUCTION

The preparation and execution of the DUNE program occupies a central position in the agenda of neutrino physics experimentation over the coming decades [1, 2]. It is natural that the first phases of the effort will focus on the short-baseline physics program at Fermilab. So far the main goal of such an effort has been to confirm or definitely, rule out the sterile neutrino hints observed in the muon neutrino beam experiments LSND and MiniBooNE [3]. While this indeed provides a strong motivation, there are others, of a more theoretical nature [4], that can further justify the efforts of a comprehensive short-baseline physics program at Fermilab [5, 6].

Amongst the strong motivations for such a dedicated neutrino program is the search for short-distance effects associated to neutrino non-unitarity, as these could possibly shed light on the underlying seesaw scale associated with neutrino mass generation [7, 8]. Current limits, as well as future expected sensitivities, have been discussed in [9–12]¹. The parameters describing nonunitary neutrino propagation have been introduced in [13, 14] for the effective case of two-neutrino mixing. A systematic generalized formalism has been presented in [17], which consistently covers all of the parameters needed to describe the case of non-unitary three-neutrino evolution. One can show that current experiments, involving only electron and muon neutrinos or anti-neutrinos can be effectively described in terms of just three new real parameters and one new CP violation phase. It has also been shown that this new phase from the seesaw mechanism brings in a new degeneracy that leads to an important ambiguity in extracting the "standard" three-neutrino phase δ_{CP} [18]. Similar ambiguities in the determination of the oscillation parameters can also appear when considering the possibility of having light sterile neutrinos [19, 20]. We discuss the potential of our proposed experimental setup for probing this scenario as well.

Recently there has been a lot of interest on the phenomenological implications of non-unitarity in laboratory searches for neutrino oscillations [9–12, 17, 18, 21–25]. In particular, ways of mitigating the effects of the above discussed ambiguity for example, by having an additional 20-ton detector in the TNT2K setup [26] has been addressed in Ref. [27]. In that case, the main motivation was the use of a cyclotron to generate a neutrino flux coming from the muon decay at rest (μ DAR) with a neutrino energy spectrum peaked around 40-50 MeV, to be detected with a 20 ton target at 20 m from the source.

Our goal in this paper is to study how the short baseline neutrino program at Fermilab could help DUNE to break the degeneracy in the measurement of the CP violation phase associated with the non-unitarity of the lepton mixing matrix. Moreover, motivated by the increased interest in Liquid Argon detectors, we have studied the perspectives of such a

¹ Astrophysical implications associated with non-unitary evolution of solar and supernova neutrinos in matter (and other, more general, non-standard interactions) have been widely discussed in the literature [13–16].

detector as a second near detector for DUNE. We have found that this setup could substantially improve the sensitivity to non-unitarity parameters. Indeed, non-unitarity manifests itself mainly as a zero-distance effect characterizing the effective non-orthonormality of the weak eigenstate neutrinos [13, 14]. As a result, improved constraints on the non-unitarity of the neutrino mixing matrix from short distance measurements would be crucial for the Long Baseline Neutrino program, as it will help to disentangle the confusion between the different CP phases appearing in the neutrino mixing matrix in the non-unitary case [17, 18].

II. BASIC SETUP

In order to introduce the notation, we briefly describe the effective parameters describing non-unitarity. The structure of the effective CC weak interaction mixing matrix is given as

$$N = N^{NP}U \quad (1)$$

where U is the standard unitary lepton mixing matrix [7] and the pre-factor matrix N^{NP} is given as [13, 14]

$$N^{NP} = \begin{pmatrix} \alpha_{11} & 0 & 0 \\ \alpha_{21} & \alpha_{22} & 0 \\ \alpha_{31} & \alpha_{32} & \alpha_{33} \end{pmatrix} \quad (2)$$

where the diagonal α_{ii} terms are real numbers and the off-diagonal entries $\alpha_{21}, \alpha_{31}, \alpha_{32}$ are in general complex. For a more detailed discussion see [17]. Constraints on the elements of U arise from global neutrino oscillation fits [28]. Laboratory sources of neutrinos are of the electron or muon-types, and these are described only by the top two rows of the new physics N^{NP} [29]. Hence the main parameter probed in our analysis is $|\alpha_{21}|^2$.

Future short-baseline neutrino experiments aiming to observe light sterile neutrinos may also be useful to obtain bounds on non-unitary parameters. In special, non-unitarity predicts a zero distance transition $\nu_\mu \rightarrow \nu_e$ [17]

$$P_{\mu e}(L=0) = \alpha_{11}|\alpha_{21}|^2, \quad (3)$$

which can be probed because the initial muon-neutrino fluxes, $\phi_{\nu_\mu}^0$, in such experiments are much larger than the electron neutrino flux contamination, $\phi_{\nu_e}^0$. Thus, at very short distances from the neutrino source, the number of detected electron neutrinos N_e is given by

$$N_e \propto \phi_{\nu_e}^0 + |\alpha_{21}|^2 \phi_{\nu_\mu}^0. \quad (4)$$

In this work we will consider two different sources of neutrinos: the Booster Neutrino Beam (BNB) and the Long-Baseline Neutrino Facility (LBNF) beam, also referred to as NUMI beam. In Fig. 1 we provide a comparison of the two Fermilab fluxes, in blue the BNB flux [6], featuring an energy peak around 0.6 GeV, and in black the LBNF flux [2] which

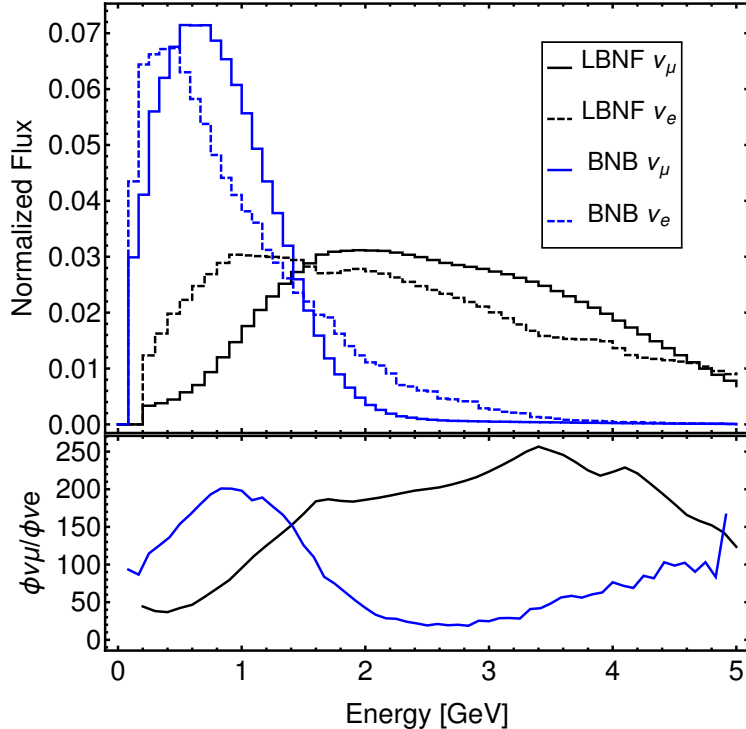


FIG. 1: Comparison between the normalized neutrino flux from the BNB (blue lines) and the LBNF/NUMI beam designed for DUNE (black lines). In the upper panel solid (dashed) lines correspond to muon (electron) neutrino fluxes.

peaks around 2 GeV. The ratio between the muon and electron neutrino fluxes is typically, $\phi_{\nu_\mu}^0/\phi_{\nu_e}^0 \sim 10^2$ in both cases, which means that one can probe differences in the detected neutrino spectrum caused by very small values of the non-unitarity parameter $|\alpha_{21}|^2$.

The current oscillation-only bound on this parameter comes mainly from the NOMAD experiment [30]

$$|\alpha_{21}|^2 < 7.0 \times 10^{-4} \text{ at 90\% C.L.} \quad (5)$$

More stringent constraints are obtained when considering charged current neutrino data. However, one should keep in mind that these limits are somewhat model-dependent.

III. THE SHORT-BASELINE PROGRAM AT FERMILAB

The Fermilab Short Baseline Neutrino Experiment (SBNE) has been designed to resolve the long-standing puzzle of light sterile neutrinos [31]. The experiment consists of three detectors at different distances: the Short Baseline Neutrino Detector (SBND), located at 110 m from the neutrino source, the MicroBooNE detector, at 470 m, and the ICARUS detector, at 600 m. Their size and characteristics are described in Table I, summarizing the SBNE proposal [5]. The neutrino source for these three detectors will be the Booster

Detector	Total Size	Active Size	Distance	Target	POT
SBND	220 t	112 t	110 m	Liq. Ar	6.6×10^{20}
MicroBooNE	170 t	89 t	470 m	Liq. Ar	1.32×10^{21}
ICARUS	760 t	476 t	600 m	Liq. Ar	6.6×10^{20}

TABLE I: Summary of the main features of the SBNE detectors [5].

Neutrino Beam (BNB) at Fermilab. Neutrino beams are generated mainly via by pion, muon and kaon decay. The pion and kaons are produced by proton collisions and the muons are generated by the pion decay. Thus, the muon neutrino flux is much bigger than the electron neutrino flux, as commented above. The BNB has already operated for several years and its flux is well understood [6]. The neutrino beam is obtained from protons extracted from the Booster accelerator, with around 5×10^{12} protons per spill hitting a beryllium target with a kinetic energy of 8 GeV [6]. This provides a neutrino flux mainly made of muon neutrinos with energies below 3 GeV and an energy distribution peaked around 600 MeV. In our analysis, the main background is the intrinsic electron neutrinos from the muon and kaon decay. Of the experiments in Table I MicroBooNE is already running, its detector has already recorded 3 years of data taking. Thus, our simulation assumes a total of 6.6×10^{20} POT for ICARUS and SBND and 1.32×10^{21} POT for MicroBooNE.

The Short Baseline Neutrino Experiment (SBNE) at Fermilab contains the necessary ingredients to observe the non-unitary muon-electron neutrino transition at short distances. It has an intense flux of muon neutrino and several detectors located at a short distance that can be sensitive to zero distance transitions such as $\nu_\mu \rightarrow \nu_e$.

The simulation of the experiment was performed by using the GLoBES package [32, 33], matching the neutrino fluxes and detector configurations to those reported in Ref. [5]. In order to include non-unitarity into the GLoBES software we have modified the build-in numerical calculation of the oscillation probability using the S -Matrix formalism described in [27]. The transition matrix $S_{\alpha\beta} = \langle \nu_\alpha | e^{-iHL} | \nu_\beta \rangle$ in the non-unitary case can be calculated by substituting the standard matter potential by $V_{\text{NU}} = (NN^\dagger)\text{Diag}[V_{CC} + V_{NC}, V_{NC}, V_{NC}](NN^\dagger)$. The conventional transition matrix S^{Unitary} of the unitary case is given through the relation

$$S = N^{NP} S^{\text{Unitary}} (N^{NP})^\dagger, \quad (6)$$

where N^{NP} is the pre-factor describing non-unitarity defined in Eq. (2).

The expected non-unitarity signal to be searched for would appear as a change in the total number of events detected with respect to that of the unitary case, and also a change in the shape of the electron neutrino spectrum. Thus, the sensitivity to the parameter $|\alpha_{21}|^2$ comes from three factors, (i) the relative size between $|\alpha_{21}|^2 \phi_{\nu_\mu}^0$ and $\phi_{\nu_e}^0$, (ii) the normalization error in the total flux and (iii) the error in the expected shape of the neutrino flux. Those are

incorporated into the simulation through the χ^2 function

$$\chi^2 = \sum_{O=1}^3 \sum_{i=1}^{N_{\text{bin}}} \left(\frac{N_{iO}^{\text{exp}} - (1 - a - a_{iO})N_{iO}^{\text{th}} - (1 - b - b_{iO})N_{iO}^{\text{bg}}}{\sqrt{N_{iO}^{\text{exp}}}} \right)^2 + \chi_{\text{SYS}}^2, \quad (7)$$

with

$$\chi_{\text{SYS}}^2 = \left(\frac{a}{\sigma_a} \right)^2 + \left(\frac{b}{\sigma_b} \right)^2 + \sum_{O=1}^3 \sum_{i=1}^{N_{\text{bin}}} \left(\frac{a_{iO}}{\sigma_{sa}} \right)^2 + \left(\frac{b_{iO}}{\sigma_{sb}} \right)^2, \quad (8)$$

where $N_{iO}^{\text{exp}} \equiv (N_{iO}^{\text{exp}})_{\text{sig}} + (N_{iO}^{\text{exp}})_{\text{bkg}}$ is the number of signal and background neutrinos at the i th-bin expected within the standard unitary 3-neutrino scenario. The subscript O runs over the three experiments (SBND, MicroBooNE and ICARUS). N_{iO}^{th} is the expected number of neutrinos for the transition $\nu_\mu \rightarrow \nu_e$ in the non-unitary case and N_{iO}^{bg} the expected number of background neutrinos, the intrinsic ν_e from the beam. Here σ_a (σ_b) is the total neutrino signal (background) uncertainty and σ_{sa} (σ_{sb}) is the shape signal (background) uncertainty. All the normalization/shape uncertainties are taken to be uncorrelated and are incorporated to the simulation through the minimization of the free parameters a, b, a_{iO} and b_{iO} for each value of $|\alpha_{21}|^2$.

The result of the simulation is presented in Fig. 2. In the left panel, we present the expected number of electron neutrino events at the ICARUS detector from the contamination of the original neutrino beam (green) and from the $\nu_\mu \rightarrow \nu_e$ signal associated to non-unitarity for $|\alpha_{21}| = 2.5\%$ (dark yellow) and for $|\alpha_{21}| = 1\%$ (light yellow). The right panel shows the expected sensitivity of the combined analysis of the SBNE experiment (combination of ICARUS, MicroBooNE and SBND detectors) to the non-unitarity parameter $|\alpha_{21}|$. In our calculations, we have assumed a 10% normalization error and a 1% shape error. With these conditions, the SBNE experiment would lead to a sensitivity of $|\alpha_{21}|^2$ at the 3×10^{-4} level, competitive with current results of non-universality searches.

IV. A SECOND NEAR DETECTOR IN THE LBNF BEAMLIN

We now consider another interesting possibility: the Fermilab Long-Baseline Neutrino Facility (LBNF) and its near detector program. As part of the future DUNE experiment [2], Fermilab's Main Injector accelerator will be used to produce the LBNF beamline, providing the highest-intensity neutrino beam in the world. In this section, we explore the potential of this new neutrino beam as a probe of the non-unitarity of the lepton mixing matrix. The DUNE experiment, supplied by the LBNF beam, will already contain a near detector, located at a distance of approximately 600 meters.

On the other hand, the ICARUS detector was constructed at CERN and brought to Fermilab to be assembled as part of the SBNE, as discussed above. Here we propose that, after finishing its operation time at SBNE, the ICARUS detector is transported again so as

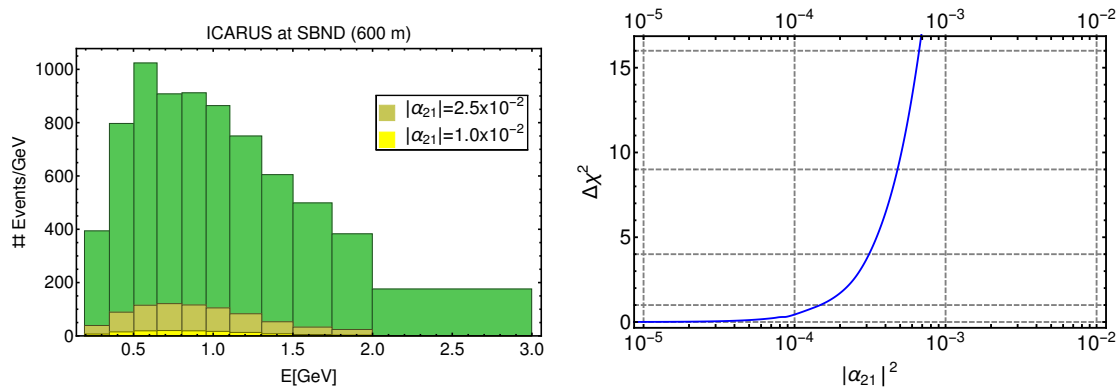


FIG. 2: **Left:** Number of electron neutrino events (in arbitrary units) expected at the ICARUS detector located at the BNB. The green histograms show events expected due to the contamination of the original neutrino beam, while those expected from the zero-distance $\nu_\mu \rightarrow \nu_e$ effect due to the non-unitarity signal are in dark yellow ($|\alpha_{21}| = 2.5\%$) and light yellow (for $|\alpha_{21}| = 1\%$). **Right:** Expected Sensitivity of SBNE to the non-unitarity parameter $|\alpha_{21}|$ assuming a 10% normalization error and a 1% shape error.

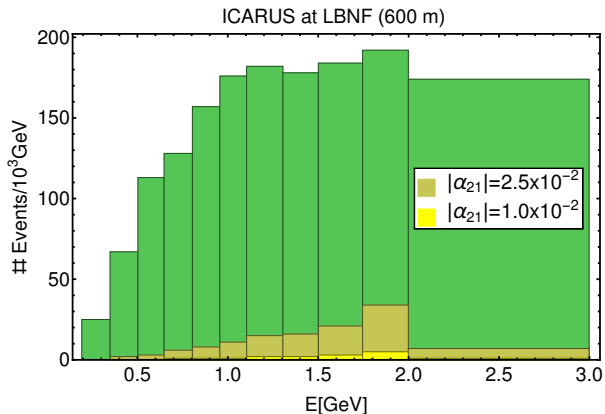


FIG. 3: Number of electron neutrino events (in arbitrary units) expected at the ICARUS detector located at 600 m of the LBNF due to the contamination of the original neutrino beam (green). We also show the expected events from a $\nu_\mu \rightarrow \nu_e$ conversion due to a non-unitarity signal given by $|\alpha_{21}| = 2.5\%$ (dark yellow) and for $|\alpha_{21}| = 1\%$ (light yellow).

to be used as a second near detector in DUNE, sitting at the LBNF neutrino beamline. As we will now show, this would be very useful in order to probe non-standard physics.

In preparing Figs. 2 and 3 we have used the fluxes given in Fig. 1. The latter gives the fluxes needed to estimate the expected event number at the ICARUS detector placed at the LBNF beamline used as the neutrino source. Notice that the number of events is much bigger at LBNF than in the BNB setup considered in Fig. 2. Nevertheless, the ICARUS detector is not optimized for the LBNF beam, since it was designed for a less energetic beam,

Detector	Active Size	Distance	E range (GeV)	Target
ICARUS	476 t	600 m	0 to 3	Liq. Argon
ICARUS+	476 t	600 m	0 to 5	Liq. Argon
protoDUNE-SP	450 t	600 m	0 to 5	Liq. Argon

TABLE II: Proposals for a second near detector in DUNE.

like the BNB beam, with neutrino energies ranging from 0 to 3 GeV with a peak around 0.6 GeV. The LBNF beamline, on the other hand, contains neutrinos from 0 to 5 GeV and peaks at 2 GeV.

In order to take into account the above features, we have considered three possible configurations for the proposed second near detector at the LBNF beam:

1. ICARUS at LBNF: This is exactly the ICARUS detector of the SBNE, working with energies between 0 to 3 GeV, located at the LBNF beamline.
2. ICARUS+ at LBNF: Again the same ICARUS detector of the SBNE, working with an extended energy window between 0 and 5 GeV and located at the LBNF beamline. In this case we have added an extra energy bin to the experiment simulation, corresponding to energies from 3 to 5 GeV. For this extra bin, we have assumed the same efficiency as in the previous energy bin.
3. A protoDUNE-like detector [34]: We have assumed the standard single phase DUNE Liquid Argon far detector configuration, with the proposed efficiency, bin size, etc and with an active mass corresponding to a 450 ton detector, as considered for the ProtoDUNE-SP detector.

There is also a 300 ton detector possibility, the Dual-Phase protoDUNE detector. Although has a smaller mass, this would employ a combination of liquid and gas Argon that may present an advantage over the standard protoDUNE Single Phase detector described above. Nevertheless, in our analysis, we will consider the simpler case of the single-phase detector, as the expected performance and design for the dual phase detector are not yet settled. A summary of these detectors can be found in Table II. Although the final design has not been fixed yet, the protoDUNE configuration described above is much more similar to what the DUNE near detector will be.

A. Sensitivity to Non-Unitarity at an LBNF near detector

The resulting sensitivity of each of the detectors proposed in Table II is plotted in Fig. 4. Here we are assuming 10% normalization error and 1% shape error. One sees that thanks to the high statistics of LBNF beam, the expected sensitivities in these cases are quite

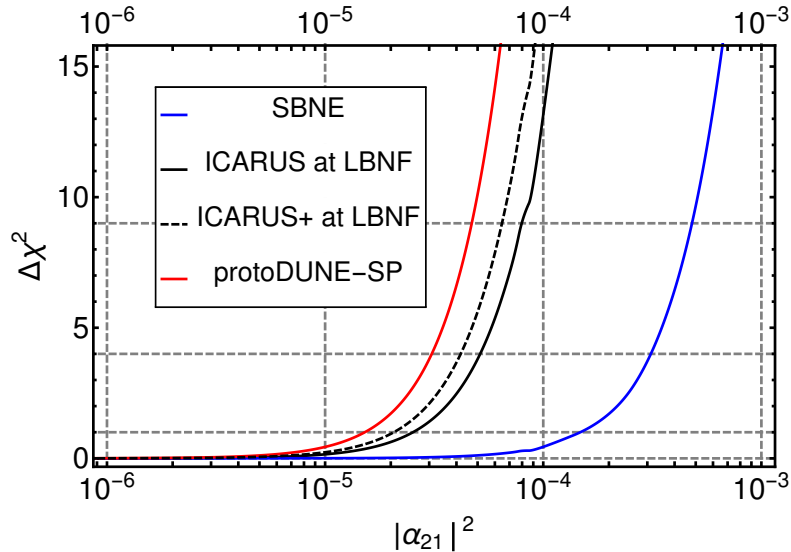


FIG. 4: Sensitivity of each configuration assumed: SBN experiment (blue), ICARUS at LBNF (black-solid), ICARUS+ at LBNF (black-dashed) and protoDUNE-SP (red). All of them are assumed to be located at 600 m from the neutrino source and running for 3.5 years in the neutrino and 3.5 in the anti-neutrino mode.

promising. Indeed, these configurations result in a substantial improvement of one order of magnitude of the sensitivity to $|\alpha_{21}|^2$.

The biggest drawback of these experiments is the requirement of knowing precisely the shape of the neutrino flux with high precision. The DUNE collaboration will predict the neutrino flux by measuring the muons and hadron-production responsible for the neutrino beam [1]. In Fig. 5 we present the sensitivity on $|\alpha_{21}|^2$ at 90% C. L. for various combinations of the baseline and the assumed uncertainty in the neutrino spectrum. Notice that the spectrum error limits the maximum attainable sensitivity on $|\alpha_{21}|^2$. For example, the protoDUNE configuration cannot reach $|\alpha_{21}|^2 < 2.5 \times 10^{-5}$ if the spectrum is not known up to a 1% precision.

The discussion of Fig. 5 can also be extended by considering the impact of the different detector sizes and distances. The results of this analysis are displayed in Fig. 6. There we have plotted the minimum requirements for obtaining a 90% C. L. bound for different values of $|\alpha_{21}|^2$ assuming a spectrum error of 1%. This figure clearly illustrates that, as expected, the smaller the detector, the closer it should be put in order to obtain a good sensitivity. Nevertheless, notice that even with a very large detector size, one can not improve the “ultimate” precision on $|\alpha_{21}|^2 < 2.5 \times 10^{-5}$ for the assumed 1% spectrum precision.

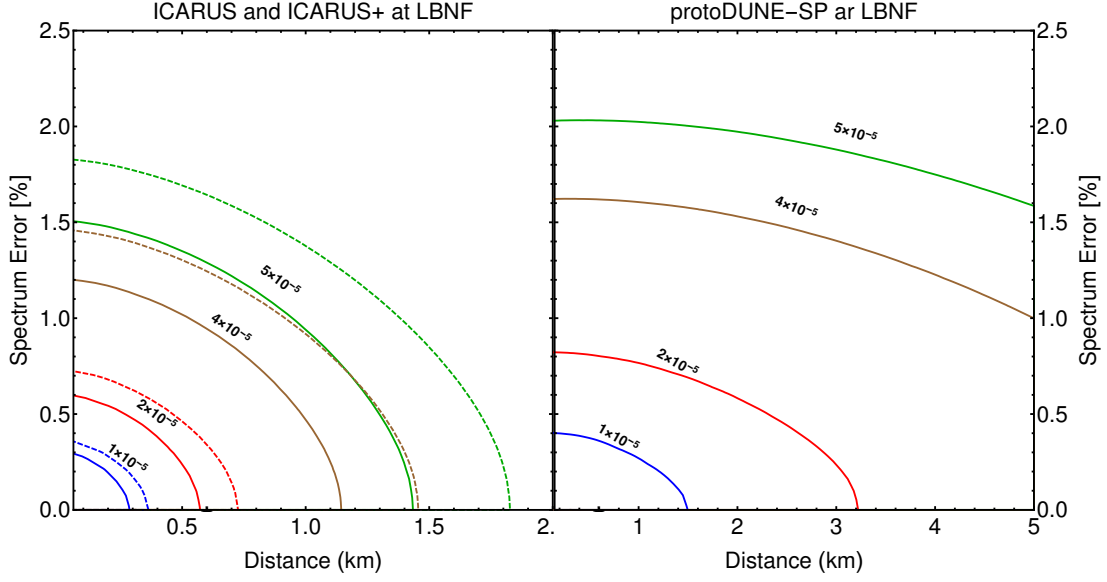


FIG. 5: **Left:** 90% C.L. sensitivity to $|\alpha_{21}|$ for ICARUS (solid line) and ICARUS+ (dashed line) for various combinations of the baseline and the spectrum error. **Right:** 90% C.L. protoDUNE-SP sensitivity for various combinations of baseline and spectrum error. Lines correspond to $|\alpha_{21}|^2 < 10^{-5}$ (blue), $|\alpha_{21}|^2 < 2 \times 10^{-5}$ (red), $|\alpha_{21}|^2 < 4 \times 10^{-5}$ (brown) and $|\alpha_{21}|^2 < 5 \times 10^{-5}$ (green).

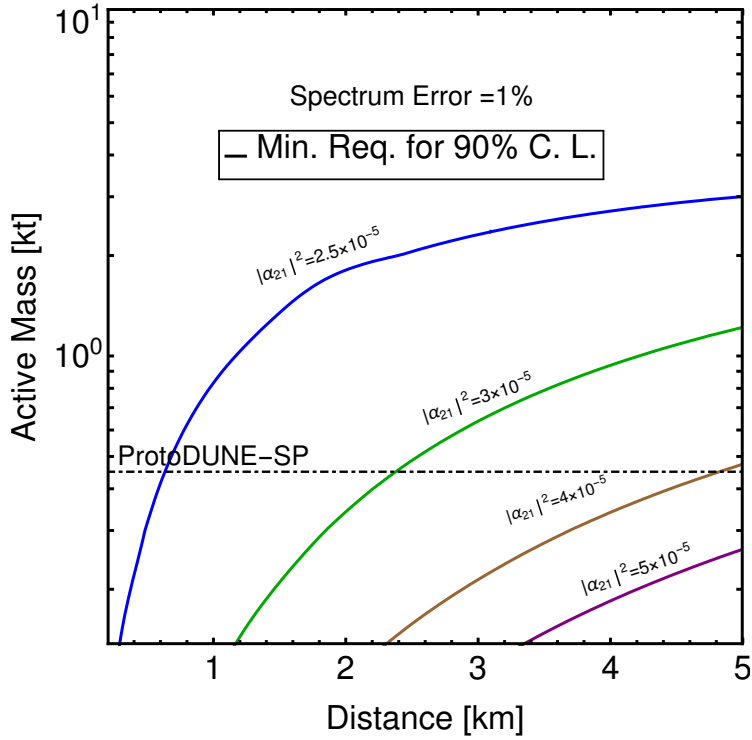


FIG. 6: Minimum detector distance and active mass requirements to attain the indicated 90% C.L. sensitivity for different values of $|\alpha_{21}|^2$, assuming an spectrum error of 1%.

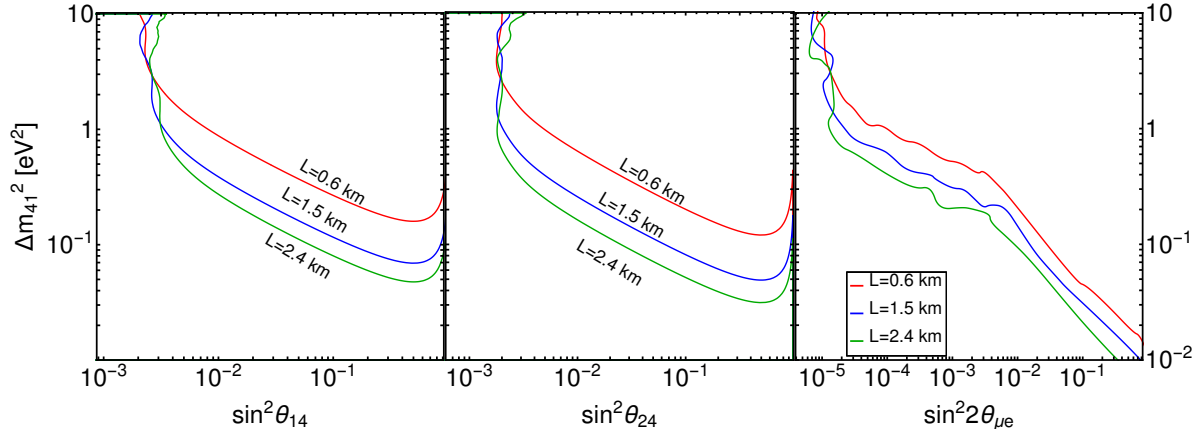


FIG. 7: ProtoDUNE-SP sensitivity at 90% CL to the 3+1 neutrino scheme for three baselines at the LBNF beam: $L = 0.6$ km (red), $L = 1.5$ km (blue) and $L = 2.4$ km (green). **Left:** $\sin^2 \theta_{14}$ versus Δm_{41}^2 **Center:** $\sin^2 \theta_{24}$ versus Δm_{41}^2 and **Right:** $\sin^2 2\theta_{\mu e}$ versus Δm_{41}^2 . A 1% spectrum error is assumed in all cases.

B. Sensitivity to light Sterile Neutrinos at an LBNF near detector

Here we focus on the short-baseline capabilities of Fermilab concerning the sensitivity to light sterile neutrinos in the eV range. The LBNF near detector will be located at around 600 m from the beam source. This opens up a possibility to probe not only zero-distance effects, but also effects that change with energy and distance, such as those associated with a light sterile neutrino. In fact, one could use one (or several) near detector(s) at the LBNF beamline in conjunction with beamline spectrum measurement to probe light sterile neutrinos. The possibility of probing sterile neutrino oscillations using a near detector in the DUNE experiment has already been considered in Ref. [35]. Although the appearance channel is in general the most sensitive, here we notice that the sensitivity to light sterile neutrinos in the disappearance channel may be substantially improved provided the uncertainty in the shape of the neutrino spectrum is good enough. To illustrate this point we consider different values of the spectrum error, as well as the possibility of combining two different near detectors in the LBNF beamline. We also pay especial attention to the effect of the distance from the source to the detector. For definiteness, we assume a 3+1 neutrino scheme, since the symmetric 2+2 schemes [36, 37] are ruled out by the solar and atmospheric neutrino oscillation data [38–40]. In the usual framework, the standard oscillation paradigm contains three active neutrinos that oscillate to one another. For a neutrino beam of energy around 2.5 GeV, a baseline of around 10^3 km would be required for the oscillation to take place. Nevertheless, the existence of one (or several) sterile neutrinos with mass-squared differences Δm_{n1}^2 , with $n > 3$, around the eV² scale would potentially give rise to oscillations in the scale of hundreds of meters.

In Fig. 7 we illustrate the effect of the baseline on the sensitivity to the 3+1 neutrino

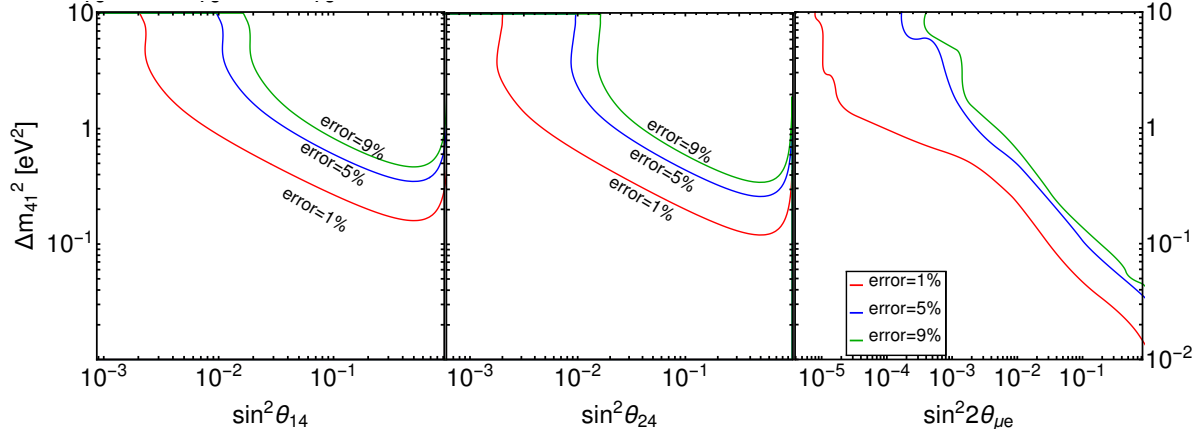


FIG. 8: Effect of the spectrum error on the at 90% CL ProtoDUNE-SP sensitivity to the 3+1 neutrino scheme for three different cases: 1% (red), 4% (blue) and 9% (green). **Left:** $\sin^2 \theta_{14}$ versus Δm_{41}^2 **Center:** $\sin^2 \theta_{24}$ versus Δm_{41}^2 and **Right:** $\sin^2 2\theta_{\mu e}$ versus Δm_{41}^2 . We have assumed a baseline of 0.6 km.

scheme of the protoDUNE-SP detector located at the LBNF beamline as proposed previously. We plot the expected sensitivity in the $\sin^2 \theta_{14}-\Delta m_{41}^2$, $\sin^2 \theta_{24}-\Delta m_{41}^2$ and $\sin^2 2\theta_{\mu e}-\Delta m_{41}^2$ planes, where $\sin^2 2\theta_{\mu e} = 4|U_{e4}|^2|U_{\mu4}|^2$. We consider different baselines and assume a 1% spectrum error. The experiment is not sensitive to θ_{34} . Fig. 8 shows the impact of the spectrum error measurement for a 0.6 km baseline protoDUNE-SP detector. In contrast to usual sterile neutrino searches, the DUNE experiment has a clear advantage, since it is sensitive to three channels: $\nu_e \rightarrow \nu_e$, $\nu_\mu \rightarrow \nu_\mu$ and $\nu_\mu \rightarrow \nu_e$. This allows one to constrain the values of θ_{14} and θ_{24} separately. In order to see this quantitatively, we have estimated the sensitivity of each disappearance channel in Figs. 7, 8 and 9. In the left panel of these figures we have focused on the electron neutrino disappearance channel, setting $\theta_{24} = 0$, while the central panel assumes $\theta_{14} = 0$ and shows the sensitivity to muon neutrino disappearance alone. The combined sensitivity on the sterile neutrino parameters coming from the disappearance channels and the appearance channel $\nu_\mu \rightarrow \nu_e$ is shown at the right panel, and has also been discussed in [35].

The usual configuration of a sterile neutrino experiment consists on a very near detector that supplies the spectrum measurement of the beamline. This could be accomplished by using the protoDUNE-like near detector at 0.6 km and the ICARUS detector at 2.4 km. This configuration improves the sensitivity to probe the 3+1 parameter space as can be seen on Fig. 9. The green line corresponds to the sensitivity curve of the protoDUNE-only configuration located at 2.4 km from the neutrino source, while the black line corresponds to the combination of ICARUS+ at 2.4 km and protoDUNE at 0.6 km. Notice that in general the combination of detectors improves the sensitivity since protoDUNE would act as a near detector for ICARUS+, providing a good estimate for the shape of the neutrino flux. Nevertheless, at $\Delta m^2 \sim 1 \text{ eV}^2$ the sensitivity of protoDUNE alone is slightly better, as

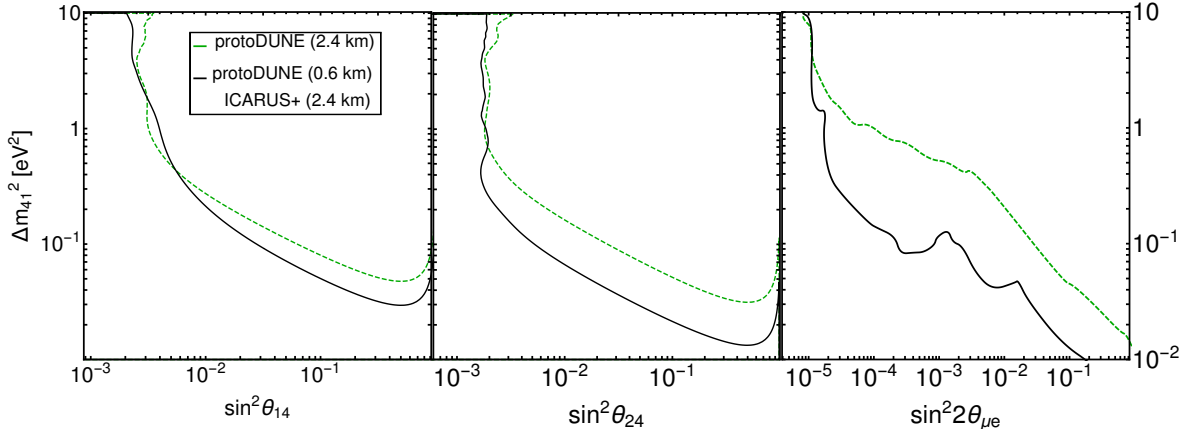


FIG. 9: The LBNF near detectors at 90% C.L. sensitivity to the 3+1 neutrino scheme is given in black for the combination of protoDUNE-SP at 0.6 km and ICARUS+ at 2.4 km. The Dashed-Green curve shows the result for the protoDUNE-only case at 2.4 km from the LBNF. **Left:** $\sin^2 \theta_{14}$ versus Δm_{41}^2 **Center:** $\sin^2 \theta_{24}$ versus Δm_{41}^2 and **Right:** $\sin^2 2\theta_{\mu e}$ versus Δm_{41}^2 . A 1% spectrum error is assumed in all cases.

2.4 km is the optimal baseline for neutrino oscillations with mass squared splitting around 1eV^2 and protoDUNE is a detector optimized for the LBNF flux.

Comparing these results with other sensitivity studies performed in the literature, for experiments such as Hyper-Kamiokande [41, 42] or MINOS+ [43, 44], one can see that the experimental setups proposed here look very promising indeed, especially for constraining $\sin^2 2\theta_{\mu e}$.

V. DISCUSSION AND CONCLUSION

We have studied the capabilities of the short baseline neutrino program at Fermilab as a probe of the unitarity of the lepton mixing matrix. In particular, we have analyzed in this case the sensitivity to the so-called zero distance effect. We have found that the sensitivity is slightly better than the current one from oscillation experiments such as NOMAD, especially when the analyses of the three upcoming detectors are combined, as shown in Fig. 2. Motivated by the future DUNE experiment, we have also analyzed the potential of different liquid Argon near detectors located in the LBNF beamline. We have found that the addition of such a near detector to the DUNE setup can substantially improve the current sensitivity on non-unitarity parameters. Fig. 4 illustrates the improvement in the sensitivity to unitarity violation that can be achieved in this case. Such improvement would help to remove the degeneracies associated with the search for CP violation at DUNE, coming from the new complex phase present in the non-unitary neutrino mixing matrix [18]. For completeness, we have also analyzed in detail how the sensitivity changes for different

configurations of baseline, mass, and systematic errors, as summarized in Figs. 5 and 6.

We have also commented on the use of such a DUNE near detector, such as a probe for light sterile neutrinos. We have studied the sensitivity of various configurations of baselines and errors (see Figs. 7 and 8). We have also studied the case (Fig. 9) of an array of two near detectors located at 0.6 and 2.4 km that could probe the $\Delta m^2 \sim 1 \text{ eV}^2$ region both for θ_{14} and θ_{24} . The impact of having a second near detector is especially visible in the expected sensitivity to $\sin^2 2\theta_{\mu e}$, plotted in the right panel of Fig. 9.

Finally, an LBNF near detector can also probe neutrino non-standard interactions (NSI). Such NSI are generically expected in neutrino mass generation schemes, not necessarily of the seesaw type [45]. Indeed, the sensitivity to NSI in the DUNE far detector has already been discussed in Refs. [46–49]. Here we stress that such interactions also lead to an effective non-unitarity-like zero-distance effect, ideal to be probed at a near detector. For the case of short-baseline neutrino experiments, matter effects in the neutrino propagation are irrelevant, and therefore the experiments are only sensitive to NSI at the neutrino production or detection processes. One can parametrize the charged current NSI at the neutrino source (s) and detection (d) in terms of two 3×3 matrices: ϵ^s and ϵ^d [50] that modify the oscillation probability to [12]

$$P_{\alpha\beta} = |[(1 + \epsilon^d)S(1 + \epsilon^s)]_{\beta\alpha}|^2, \quad (9)$$

where S is the propagation matrix. The limit $\epsilon^a \rightarrow 0$, with $a = s, d$, restores the standard oscillation result. The analogue zero-distance effect corresponding to Eq. (4) becomes

$$N_e \propto |(1 + \epsilon_{ee}^s)(1 + \epsilon_{ee}^d) + \epsilon_{e\mu}^d \epsilon_{\mu e}^s|^2 \phi_{\nu_e} + |(1 + \epsilon_{ee}^s)\epsilon_{e\mu}^d + (1 + \epsilon_{\mu\mu}^d)\epsilon_{e\mu}^s|^2 \phi_{\nu_\mu} \quad (10)$$

Therefore, all the analyses obtained before can be extended to cover this case as well, by substituting $|\alpha_{21}|^2$ by the quantity,

$$|\alpha_{21}|^2 \rightarrow \frac{|(1 + \epsilon_{ee}^s)\epsilon_{e\mu}^d + (1 + \epsilon_{\mu\mu}^d)\epsilon_{e\mu}^s|^2}{|(1 + \epsilon_{ee}^s)(1 + \epsilon_{ee}^d) + \epsilon_{e\mu}^d \epsilon_{\mu e}^s|^2} \approx |\epsilon_{e\mu}^d + \epsilon_{e\mu}^s|^2 \quad (11)$$

Notice that the experiment becomes blind to NSI in the special case $\epsilon_{\mu e}^d \approx -\epsilon_{\mu e}^s$.

In summary, our main point in this paper has been to stress the importance of probing short distance physics through the use of near detectors in DUNE. We have illustrated the physics that can be probed in several different configurations. In order to bring the issue to the experimental agenda we have proposed idealized benchmarks and determined their physics reach. Our results should trigger discussion in the community and help choose an optimized and realistic option. Dedicated scrutiny will be needed in order to design the ultimate setup to be chosen, in view of its physics interest as well as technical feasibility.

Acknowledgments

The authors would like to thank G. V. Stenico for providing the SBND GloBES code for the detectors. Work supported by the Spanish grants FPA2017-85216-P and SEV-2014-0398 (MINECO), PROMETEOII/2014/084 and GV2016-142 grants from Generalitat Valenciana. MT is also supported a Ramón y Cajal contract (MINECO). OGM was supported by CONACyT and SNI (Mexico). P. P. thanks the support of FAPESP-CAPES funding grant 2014/05133-1, 2014/19164-6 and 2015/16809-9 Also the partial support from FAEPEX funding grant, No 2391/17.

-
- [1] R. Acciarri et al. (DUNE) (2016), 1601.02984.
 - [2] R. Acciarri et al. (DUNE) (2015), 1512.06148.
 - [3] J. M. Conrad, W. C. Louis, and M. H. Shaevitz, *Ann. Rev. Nucl. Part. Sci.* **63**, 45 (2013), 1306.6494.
 - [4] H. Nunokawa, S. J. Parke, and J. W. Valle, *Prog.Part.Nucl.Phys.* **60**, 338 (2008), 0710.0554.
 - [5] A. M. Szelc (SBND), *JINST* **11**, C02018 (2016).
 - [6] M. Antonello et al. (LAr1-ND, ICARUS-WA104, MicroBooNE) (2015), 1503.01520.
 - [7] J. Schechter and J. W. F. Valle, *Phys. Rev.* **D22**, 2227 (1980).
 - [8] O. G. Miranda and J. W. F. Valle, *Phys.Rev.* **D62**, 113012 (2000), hep-ph/0008114.
 - [9] E. Fernandez-Martinez, M. B. Gavela, J. Lopez-Pavon, and O. Yasuda, *Phys. Lett.* **B649**, 427 (2007), hep-ph/0703098.
 - [10] S. Antusch and O. Fischer, *JHEP* **10**, 094 (2014), 1407.6607.
 - [11] F. J. Escrihuela, D. V. Forero, O. G. Miranda, M. Tórtola, and J. W. F. Valle, *New J. Phys.* **19**, 093005 (2017), 1612.07377.
 - [12] M. Blennow, P. Coloma, E. Fernandez-Martinez, J. Hernandez-Garcia, and J. Lopez-Pavon, *JHEP* **04**, 153 (2017), 1609.08637.
 - [13] J. W. F. Valle, *Phys. Lett.* **B199**, 432 (1987).
 - [14] H. Nunokawa, Y. Z. Qian, A. Rossi, and J. W. F. Valle, *Phys. Rev.* **D54**, 4356 (1996), hep-ph/9605301.
 - [15] A. Esteban-Pretel, R. Tomas, and J. W. F. Valle, *Phys. Rev.* **D76**, 053001 (2007), 0704.0032.
 - [16] C. S. Fong, H. Minakata, and H. Nunokawa (2017), 1712.02798.
 - [17] F. J. Escrihuela, D. V. Forero, O. G. Miranda, M. Tortola, and J. W. F. Valle, *Phys. Rev.* **D92**, 053009 (2015), 1503.08879.
 - [18] O. G. Miranda, M. Tortola, and J. W. F. Valle, *Phys. Rev. Lett.* **117**, 061804 (2016), 1604.05690.
 - [19] S. Choubey, D. Dutta, and D. Pramanik, *Phys. Rev.* **D96**, 056026 (2017), 1704.07269.
 - [20] S. K. Agarwalla, S. S. Chatterjee, and A. Palazzo (2018), 1801.04855.

- [21] S. Goswami and T. Ota, Phys. Rev. **D78**, 033012 (2008), 0802.1434.
- [22] J. Kopp, T. Ota, and W. Winter, Phys. Rev. **D78**, 053007 (2008), 0804.2261.
- [23] D. Dutta, P. Ghoshal, and S. K. Sehrawat (2016), 1610.07203.
- [24] D. Dutta, P. Ghoshal, and S. Roy, Nucl. Phys. **B920**, 385 (2017), 1609.07094.
- [25] D. Dutta and P. Ghoshal, JHEP **09**, 110 (2016), 1607.02500.
- [26] S.-F. Ge and A. Yu. Smirnov, JHEP **10**, 138 (2016), 1607.08513.
- [27] S.-F. Ge, P. Pasquini, M. Tortola, and J. W. F. Valle, Phys. Rev. **D95**, 033005 (2017), 1605.01670.
- [28] P. F. de Salas et al. (2017), 1708.01186.
- [29] C. Patrignani et al. (Particle Data Group), Chin. Phys. **C40**, 100001 (2016).
- [30] P. Astier et al. (NOMAD), Phys. Lett. **B570**, 19 (2003), hep-ex/0306037.
- [31] K. N. Abazajian et al. (2012), 1204.5379.
- [32] P. Huber, M. Lindner, and W. Winter, Comput. Phys. Commun. **167**, 195 (2005), hep-ph/0407333.
- [33] P. Huber, J. Kopp, M. Lindner, M. Rolinec, and W. Winter, Comput. Phys. Commun. **177**, 432 (2007), hep-ph/0701187.
- [34] L. Manenti, in *Proceedings, Prospects in Neutrino Physics (NuPhys2016): London, UK, December 12-14, 2016* (2017), 1705.05669.
- [35] S. Choubey and D. Pramanik, Phys. Lett. **B764**, 135 (2017), 1604.04731.
- [36] J. T. Peltoniemi, D. Tommasini, and J. W. F. Valle, Phys. Lett. **B298**, 383 (1993).
- [37] J. T. Peltoniemi and J. W. F. Valle, Nucl. Phys. **B406**, 409 (1993), hep-ph/9302316.
- [38] M. Maltoni, T. Schwetz, M. A. Tortola, and J. W. F. Valle, New J. Phys. **6**, 122 (2004), hep-ph/0405172.
- [39] J. Kopp, P. A. N. Machado, M. Maltoni, and T. Schwetz, JHEP **05**, 050 (2013), 1303.3011.
- [40] S. Gariazzo, C. Giunti, M. Laveder, and Y. F. Li, JHEP **06**, 135 (2017), 1703.00860.
- [41] K. J. Kelly, Phys. Rev. **D95**, 115009 (2017), 1703.00448.
- [42] J. Tang, Y. Zhang, and Y.-F. Li, Phys. Lett. **B774**, 217 (2017), 1708.04909.
- [43] G. Tzanankos et al. (MINOS+) (2011).
- [44] P. Adamson et al. (MINOS), Submitted to: Phys. Rev. Lett. (2017), 1710.06488.
- [45] S. M. Boucenna, S. Morisi, and J. W. F. Valle, Adv. High Energy Phys. **2014**, 831598 (2014), 1404.3751.
- [46] M. Masud, M. Bishai, and P. Mehta (2017), 1704.08650.
- [47] A. de Gouvea and K. J. Kelly (2015), 1511.05562.
- [48] P. Coloma, JHEP **03**, 016 (2016), 1511.06357.
- [49] J. Liao, D. Marfatia, and K. Whisnant, JHEP **01**, 071 (2017), 1612.01443.
- [50] Y. Farzan and M. Tortola (2017), 1710.09360.